Conceptual design and supporting analysis of a double wall heat exchanger for an ARC-class fusion reactor Primary cooling system

Fusion Engineering and Design 201 (2024) 114261

Contents lists available at ScienceDirect

Fusion Engineering and Design

journal homepage: www.elsevier.com/locate/fusengdes

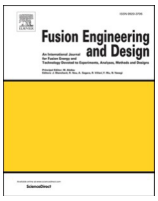

Conceptual design and supporting analysis of a double wall heat exchanger for an ARC-class fusion reactor Primary cooling system

Francesco Colliva [a,*], Federico Hattab [a], Simone Siriano [a], Gabriele Ferrero [b], Samuele Meschini [b], Raffaella Testoni [b], Massimo Zucchetti [b], Andrea Iaboni [c], Giulia Valeria Centomani [c], Antonio Trotta [c], Cristiano Ciurluini [a]

[a] Sapienza University of Rome, DIAEE – Nuclear section, Corso Vittorio Emanuele II 244, 00186 Rome, Italy
[b] Politecnico di Torino, Dep. Of Energy "Galileo Ferraris", 10129 Turin, Italy
[c] MAFE, Eni S.p.A, 30175 Venice, Italy

ARTICLE INFO

Keywords:
Arc
Double wall heat exchanger
Tritium
FLiBe
RELAP5-3d©
OpenFOAM

ABSTRACT

In the fight against climate change through the progress of fusion technology, the Affordable, Robust and Compact (ARC) fusion reactor design is under development at Commonwealth Fusion Systems (CFS) and Massachusetts Institute of Technology (MIT)- Plasma Science and Fusion Center, in collaboration with the Ente Nazionale Idrocarburi (ENI) S.p.A. The reactor features demountable superconducting toroidal field coils and a replaceable vacuum vessel immersed in a Fluorine Lithium Beryllium (FLiBe) molten salt blanket. The low-pressure molten salt cools the divertors and the blanket, shields the magnets and acts as tritium breeder and tritium carrier. Tritium must be recovered efficiently from the salt to fuel the reactor, minimizing its inventory and its migration outside the FLiBe loop. The current work is aimed at presenting a preliminary design of a Double-Wall Heat eXchanger (DWHX) to be installed in an ARC-class reactor primary cooling system. The main feature is the presence of a flowing sweep gas gap which captures tritium and prevents its diffusion toward the secondary system. For the DWHX, thermal-hydraulic and tritium transport analyses were performed, considering a supercritical water Rankine power conversion system on the secondary side to carry out the calculations. To assess tritium extraction capabilities of the DWHX, the tritium extraction efficiency has been evaluated. Calculation results highlighted how the current configuration is not adequate to remove tritium, in fact the tritium extraction efficiency is very low. On the other side, it seems to act adequately as tritium permeation barrier.

1. Introduction

An ARC reactor represents one of the studied solutions for fusion devices, to make fusion energy convenient and economically competitive with respect to other energy sources [1]. This reactor has been proposed by the MIT Plasma Science and Fusion Center and developed by CFS.

An ARC-class tokamak fusion reactor foresees the use of FLiBe molten salt as primary fluid, which acts at the same time as coolant, neutron shield, tritium breeder and tritium carrier [2,3]. When producing the FLiBe, lithium may be enriched of the isotope Li^6, which has a much larger (n,2n) cross section below 1 MeV compared to Li^7 and is the main contributor to tritium generation. The production of tritium within molten salt leads the need to collect the tritium from the FLiBe for use as fuel and prevent its permeation into the Power Conversion System, which is currently under study [4], to ensure compliance with regulatory limits [5]. Indeed, results from ARC fuel cycle modeling showed the presence of large tritium losses due to non-radioactive phenomena (e.g., fractions of tritium inventory > 10–4 [6]), through the system rapidly make tritium self-sufficiency unattainable and tritium release unacceptable from the safety viewpoint [6]. Within the heat exchanger, due to the large and thin surfaces required for heat transfer, special attention is needed to avoid excessive tritium losses towards the secondary system. Several transport mitigation strategies have been proposed [7]. Among these, there are preliminary designs of DWHX proposed and investigated in [5] and [8]. For the purpose of the current study, the Balance of Plant (BoP) is assumed to be a supercritical Rankine cycle because this solution is the best from the point of view of the BoP

* Corresponding author.
E-mail address: francesco.colliva@uniroma1.it (F. Colliva).

https://doi.org/10.1016/j.fusengdes.2024.114261
Received 10 October 2023; Received in revised form 12 January 2024; Accepted 13 February 2024
Available online 16 February 2024

efficiency and the commercial availability, as discussed in [4]. The use of different power cycles may impact tritium transport within the heat exchanger (i.e., due to a different secondary fluid). However, the need to prevent contamination of the secondary fluid remains applicable regardless of the chosen power cycle.

The aim of this work is to evaluate the performances of a DWHX both as a heat exchanger that acts as a tritium barrier towards the secondary system and as a Tritium Extraction System (TES). To do so, it is assumed that the FLiBe exiting the blanket is sent directly to the DWHX, without any passage through an eventual TES (still to be designed). Thermal-Hydraulic (TH) and tritium transport analyses were performed. The thermal-hydraulic analysis was carried out with the software RELAP5-3D©, a best estimate thermal-hydraulic code that allows the simulation of system behavior both in steady-state and transient conditions [9]. First, a reference preliminary HX design was studied. Then, some sensitivity studies were performed with the aim of the design improvement. Results obtained through RELAP5-3D© simulations were used as input data for the tritium transport analysis.

Tritium transport within the HX was numerically investigated by Computational Fluid Dynamics (CFD) simulations using a custom solver of OpenFOAM, an open-source CFD toolbox [10]. Tritium release rates to the helium flowing in the gap and to the secondary supercritical water were computed, allowing the evaluation of the DWHX tritium barrier and extraction efficiencies.

This paper is divided into several chapters. After the current introduction, Chapter 2 provides the detailed description of the DWHX thermal-hydraulic analysis performed with RELAP5-3D© system code. The outcomes of this study were used to carry out the tritium transport analysis presented in Chapter 3. The main conclusions of the overall work are drawn in Chapter 4.

2. DWHX thermal-hydraulic analysis

2.1. Reference case

The ARC primary cooling system is assumed to be constituted by three parallel circuits, each one provided with a 210 MWth DWHX. The heat exchangers are equipped with double wall tubes, as shown in Fig. 1, which main parameters related to the preliminary design are collected in Table 1. In Fig. 1 OD represents the outer diameter of tubes, while t represents their thickness. Primary and secondary fluids flow in countercurrent: water moves upwards in the inner tube (in green), while FLiBe goes downwards in the shell side (in red). Fluids are separated by a gap filled with helium, which flows upward (in yellow). The preliminary value selected for the helium thickness is reported in Table 1. The reference thermodynamic conditions for FLiBe were derived from [3]. They are also collected in Table 1.

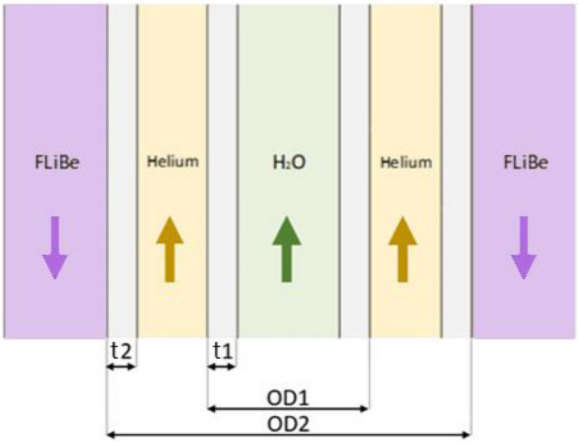

Fig. 1. Double Wall Tube radial section.

Table 1
Input parameters for the DWHX sizing.

Parameter	Unit	Value
OD1	mm	19.05
OD2	mm	25.40
t1	mm	4.25
t2	mm	1.88
He gap thickness	Mm	1.30
Thermal Power	MW	210
Inlet H_2O Temperature	K	593.15
Outlet H_2O Temperature	K	853.15
Outlet H_2O Pressure	Bar	250
H_2O Mass Flow	kg/s	105
Inlet FLiBe Temperature	K	908.15
Outlet FLiBe Temperature	K	800.15
Outlet FLiBe Pressure	Bar	10
FLiBe Mass Flow	kg/s	815

Primary and secondary fluids mass flow rates are evaluated through a power balance, using thermal power and inlet/outlet temperatures, and are reported in Table 1. In contrast, helium mass flow rate is preliminarily assessed by considering, at the HX outlet, a maximum velocity of 40 m/s and a maximum temperature of 880 K. These values are assumed as sizing criteria. The helium gap cross area is calculated by using data in Table 1. The thermodynamic properties for FLiBe, H_2O and He are derived respectively from [11,12] and [13]. It should be noted that in order to obtain an acceptable HX geometrical layout (in terms of height and footprint), a high helium flow must be adopted (to reduce the corresponding thermal resistance that is the dominant one in the HX). This allows to reduce the insulation effect operated by the gas. At a later stage of the ARC design, a system to recover the thermal power removed by helium will be studied. This solution will be integrated with the strategy to separate the tritium extracted by the gas within the HX (see Section 3).

Starting from data in Table 1, a preliminary sizing of the HX was performed whose results are reported in Table 2. To assess the Heat Transfer Coefficient (HTC) for supercritical water, Dittus-Boelter correlation [14] was adopted, while Gnielinski formulation [15] was used for the helium and FLiBe working fluids.

To verify the TH design, a numerical simulation was run by using the best-estimate system code RELAP5-3D©. A simplified model of the primary circuits is adopted (see Fig. 2). Volumes and junctions are identified by numbers: 1-xx components contain water, 2-xx. Helium and 3-xx FLiBe. The primary circuit model contains a lumped model of the Breeding Blanket, the pressure control function, and the primary pipelines. For the BB, the overall thermal inertia, and the FLiBe Inventory (250 m^3) were kept. Referring to the primary pipelines, an approximate length value (30 m) was derived by making some preliminary assumptions on the ARC tokamak building [1]. The pipeline internal diameter (0.4 m) was assessed by considering a limit velocity for FLiBe of 3 m/s. This has been chosen in order to avoid problem related to corrosion effects. The pressure control function was designed to keep the primary pressure (see Table 1). It consists of a tank with FliBe covered by an inertial gas. The primary pressure is maintained around the nominal value through two valves, one injects and one discharges the inertial gas

Table 2
DWHX sizing: output parameters for reference case.

Parameter	Unit	Value
Height	m	18.3
Tubes number	/	4000
Average overall HTC	W/(m^2K)	235.2
Inlet He Temperature	K	695.8
Outlet He Temperature	K	880.7
He Pressure	bar	50
He Mass Flow	kg/s	34.7
Bundle p/d (pitch/diameter)	/	1.2

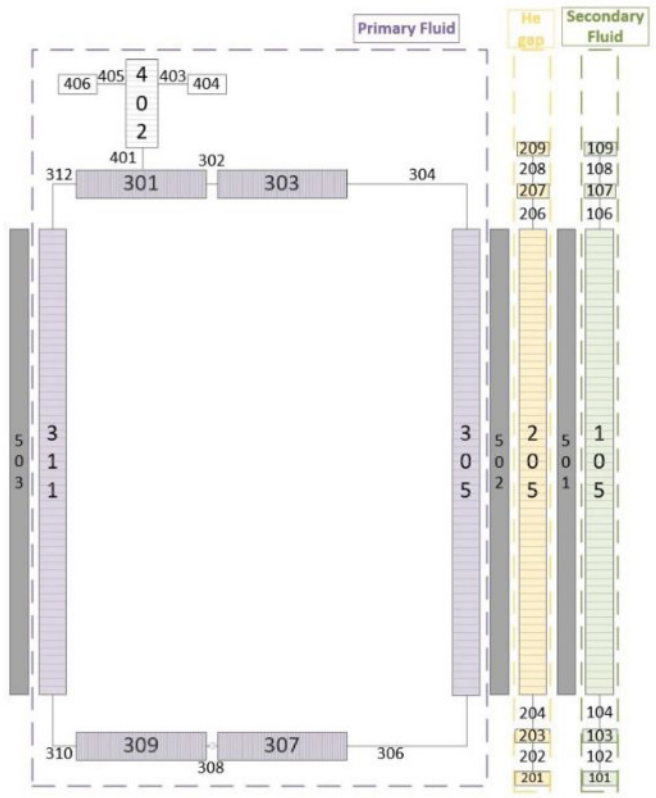

Fig. 2. ARC primary cooling system: RELAP5-3D© nodalization.

as answer to a decrease or increase of pressure, respectively. Only one loop (of three) was considered in the input deck since they have the same TH behavior. Concerning the heat exchanger, double wall tubes were modelled with equivalent pipe components. They are characterized by the flow area and the mass flow of the entire bundle, the total tube length and the hydraulic diameter of the single tube. This modelling approach allows to correctly evaluate both the pressure drops and heat transfer phenomena. It was already successfully adopted in other works concerning simulations of fusion reactor primary cooling systems [16, 17]. More in detail, double wall tubes are simulated through three pipes (representing the fluid domains) connected by two heat structures (simulating the inner/outer tubes). For water and helium, the inlet temperature and outlet pressure were imposed as boundary conditions, as well as the helium mass flow. Time-dependent volumes and junctions were used for this purpose. The FLiBe mass flow rate circulating into the primary loop was set by means of a time-dependent junction, preliminary simulating the presence of a pump (whose design is still to be performed at this stage of the ARC design). A control system was introduced in the RELAP5-3D© input deck to match the design FLiBe temperature at the DWHX outlet (i.e., at the BB inlet) since it is a requirement for the ARC primary cooling system operation. It used the supercritical water mass flow rate as controlled parameter.

As shown by Table 3, the numerical results are in good accordance with the design data, verifying the appropriateness of the DWHX thermal-hydraulic design. Between brackets, the errors with respect to the nominal values are reported, for the parameters not set as boundary conditions. The only deviations were observed for the supercritical water. For the latter, the value predicted by the code is higher than the nominal one, see Table 3. As a consequence of the power balance, the outlet temperature is lower. This is mainly due to the fact that RELAP5-3D© computes a water average HTC that is lower than the one assessed during the HX sizing calculation. According to the code manual [9], the correlation used should be Dittus-Boelter, the same used to obtain the results in Table 2. For this reason, this aspect is still under investigation.

Table 3
Reference case: RELAP5-3D© outcomes.

Parameter	Unit	Value
HX Exchanged Power	MW	210 (0 %)
Inlet H_2O Temperature (BC*)	K	593.15
Outlet H_2O Temperature	K	829.4 (−23 K)
H_2O Mass Flow Rate	kg/s	112 (6.7 %)
Outlet H_2O Pressure (BC*)	Bar	250
Inlet FLiBe Temperature	K	907.6 (−0.55 K)
Outlet FLiBe Temperature	K	800.2 (+0 K)
FLiBe Mass Flow Rate (BC*)	kg/s	814.9
Inlet FLiBe Pressure	bar	10.1 (+1 %)
Inlet He Temperature (BC*)	K	695.8
Outlet He Temperature	K	879.6 (−1.05 K)
He Mass Flow Rate (BC*)	kg/s	34.7
Outlet He Pressure (BC*)	bar	50

BC*: imposed as boundary condition.

2.2. Sensitivity analysis

To optimize the DWHX TH design, a sensitivity study was carried out involving some selected parameters. In Table 4 the varied parameters are reported, together with the resulting overall HX HTC (Avg U) and component height, which varies to keep the power processed by the HX constant (see Table 3). In addition, Fig. 3 shows how the parameters variation influences the total thermal resistance (R''). As visible from the figure, the main contribution is due to the FLiBe, due to its low velocity within the HX bundle. For this, a very small value for the bundle p/d was selected for the reference case (see Table 2). The technical feasibility and manufacturability of a tubesheet characterized by such a small value of p/d must be still checked. However, the increase of this parameter (see case S1 in Table 4) produces a significant increment of the component height. Referring to the helium, its high flow rate positively affects the overall HX heat transfer by reducing the corresponding thermal resistance. As a consequence, when this parameter is reduced/increased (see cases S2 and S3 in Table 4) an inverse effect can be envisaged for the tube length. What is interesting to note is also the influence of the helium pressure. If it is reduced (case S4 in Table 4), the fluid density is accordingly lowered producing a reduction of the fluid heat transfer capability (i.e., increase of the required HX heat transfer surface). Some scoping calculations were also performed by varying the HX tube design. Case S5 refers to an increase of the external tube diameter (OD2 in Fig. 1) with unaltered internal tube, helium gap and bundle pitch. In this case, the FLiBe flow area decreases, leading to a rise of the corresponding fluid velocity and HTC, and resulting in a shorter HX height. Although, this solution is not recommendable since p/d is even lower than the one in Table 2. The same occurs when the He gap thickness is increased (the new OD2 value is 28.6 mm). In the case S7, the internal tube is reduced keeping constant the helium gap and the external tube thickness (the new OD2 value is 22.2 mm). In this case, since the FLiBe

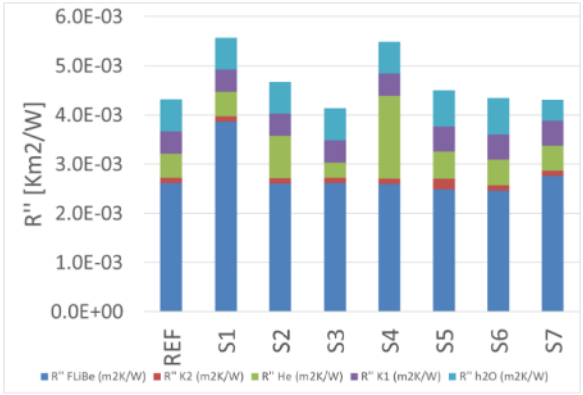

Fig. 3. Contributions to the total thermal resistance.

Table 4
List of sensitivity analysis.

Case ID #	Name	Sensitivity parameter		Avg HTC (W/(m^{2}K))	HX height (m)
		Ref value	New value		
REF	–	–	–	235.2	18.3
S1	p/d	1.2	1.3	180.9	23.7
S2	Max He velocity	40 m/s	20 m/s	216.8	19.9
S3	Max He velocity		70 m/s	245.7	17.6
S4	He pressure	50 bar	10 bar	184.0	23.3
S5	OD2	25.4 mm	28.6 mm	226.4	17
S6	He gap	1.3 mm	2.9 mm	235.1	16.4
S7	OD1	19.05 mm	15.9 mm	233.1	20.9

flow area increases, the effect on the HX height is opposite.

In addition to the reference case, cases S2 and S3 (characterized by a decrease/increase of He velocity, respectively) were selected to be investigated in detail with the RELAP5-3D© code and to perform tritium transport analysis. Fig. 4 shows the temperature profiles along the tube length for the three fluids (water, Helium and FLiBe). Trends are sorted from the HX bottom to top (i.e., co-current with water and helium). Since the three cases are characterized by different HX height, to enhance the Fig. 4 readability, the normalized coordinate is used for the x-axis. It can be seen how a reduction of He velocity (case S2) causes an increase of its resistance to the heat transfer, reducing its temperature and the H_2O one. On the contrary, an increase of He velocity (case S3) causes an increase in heat transfer, resulting in higher He and H_2O temperatures. These trends are used as input data for the tritium transport analysis.

Referring to cases S5 to S7, the main element affecting the results is the variation of the FLiBe flow area produced by the modification of the selected parameter. To better highlight the actual influence of the tube parameters on the HX design, in the future development of the activity, further cases will be studied and added to the presented sensitivity where the FLiBe flow area will be kept constant while varying the tube design.

3. Tritium transport calculations

3.1. Code features and methods

OpenFOAM is a free, open-source CFD software containing many solvers used to reproduce various physical problems. Among these, *chtMultiRegionFoam* is a transient fluid flow and solid heat conduction solver, capable of simulating conjugate heat transfer between regions, buoyancy effects, turbulence, chemical reactions and radiation modelling [10]. Conjugate heat transfer between fluid and solid regions is carried out using a coupling Boundary Condition (BC), which ensures temperature continuity and heat flux conservation across the interface between the different computational domains [10].

In this work, the tritium transport inside the DWHX of an ARC-class reactor has been modelled using a custom version of the solver and coupling BC. The developed numerical model has been extensively verified and validated with several benchmarks, including analytical [18–23], experimental [24–26], and other numerical data [27–29]. The code was able to accurately reproduce the tritium transport and permeation physics, in both the Diffusion Limited Regime (DLR) and Surface Limited Regime (SLR) and also considering tritium trapping. Interested readers can find a detailed description of how the developed code works and the V&V results in ref [30]. In this solver the tritium concentration (C, mol/m^3) is added as a scalar field, along with diffusion coefficients (D, m^2/s) and solubilities. In each region the T_2 transport

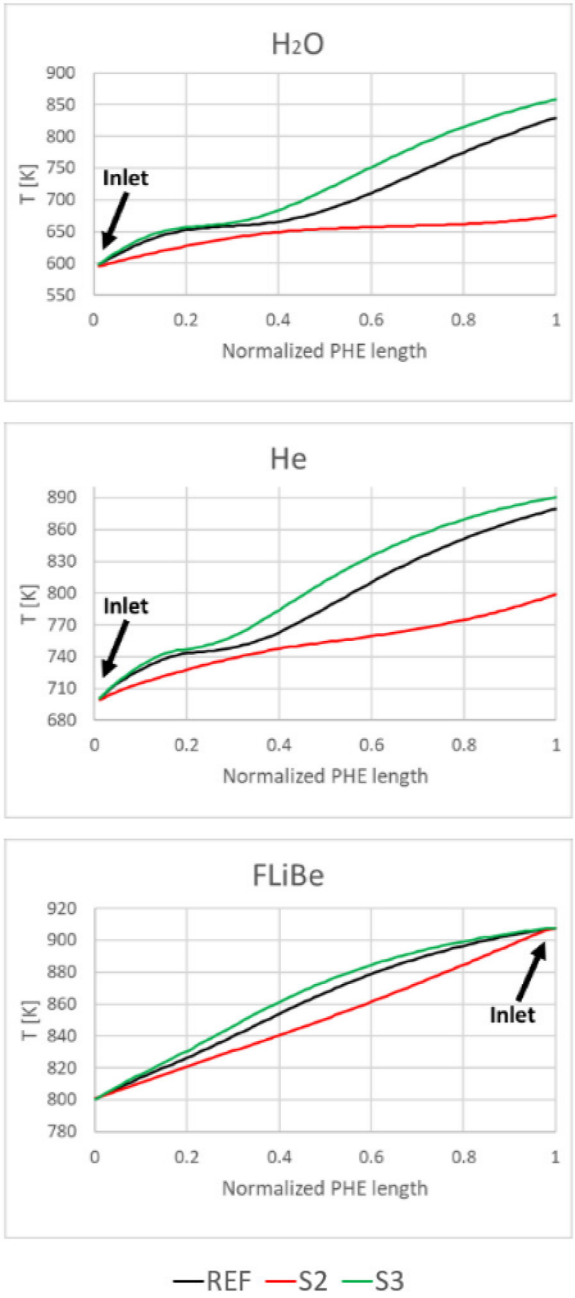

Fig. 4. Fluids temperature profiles.

scalar equation has been implemented solving the purely diffusive process in the solid regions and the combined diffusive-convective process in the fluid ones, as shown in eq. (1), where $\vec{U}$ (m/s) is the velocity field and S_c is a volumetric source term (mol/s). Hydrogen partial pressure is derived from the computed concentration, using the solubilities.

$$\frac{\partial C}{\partial t} + \nabla\cdot\left(\vec{U}C\right) - \nabla\cdot(D\nabla C) = S_C \tag{1}$$

The BC used for coupling the tritium transport between solid and fluid regions works under the assumption of diffusion-limited transport (i.e., the permeation is limited by diffusion and mass transport phenomena and not by surface effects at fluid-metal interfaces [31]) and ensures the continuity of tritium partial pressure (P, Pa) and the conservation of tritium fluxes (J, mol/m^{2}s) at the region interfaces, as shown in the Eqs. (2),(3) below:

$$P_1 = P_2 \tag{2}$$

$$J_1 = J_2 \rightarrow -D_1\frac{\partial C_1}{\partial n_1} = -D_2\frac{\partial C_2}{\partial n_2} \tag{3}$$

Where n is the normal to the wall. Tritium solubility in FLiBe and in Helium is described by Henry's law [32,33] ($K_{fluid}, mol/(m^3\ Pa)$), while in metals by Sieverts' law [33] ($K_{solid}, mol/(m^3\ \sqrt{Pa})$). Pedices 1 and 2 indicate the parameters belonging to the two sides of a given interface between two regions. Thus, for an interface between a fluid and a solid, Eq. (2) can be written as:

$$\frac{C_{fluid}}{K_{fluid}} = \left(\frac{C_{solid}}{K_{solid}}\right)^2 \tag{4}$$

It should be noted that another difference in tritium transport in solids and the fluids is that diffusion is atomic in the former (T) and molecular in the latter (T_2). For easier accounting the notation T_2 is used throughout the entire domain.

3.2. Physical and numerical model

The simulation domain is a 2D representation of half of the radial section of one double-walled tube of the heat exchanger, along its entire length. This modeling approach is chosen to limit computational cost due to the significant length of the component. The assumption of no dedicated TES upstream the DWHX is conservative with respect to the calculation of the amount of tritium lost from the primary FLiBe. No volumetric source terms are considered (source term in Eq. (1) is equal to zero), the only source of tritium is at the inlet of the FLiBe flow. Such inlet source term is assumed to be constant in time and does not account for pulsed operation of the fusion device. Permeation is assumed to be diffusion limited and all tritium in FLiBe is assumed to be in molecular form (T_2), thus representing an upper limit of the tritium concentration in the salt. There are four regions: inner wall (w1), helium, outer wall (w2) and FLiBe (see Fig. 5). Under the assumption that there is no dedicated TES and that the FLiBe exiting the blanket is sent directly to the DWHX, a tritium concentration of 1.36E-04 mol/m^3 is imposed at the DWHX FLiBe inlet and is derived from ref. [34]. The regions boundaries in the radial direction are coupled with the custom BC described in the previous section. Instead, at the w1 left boundary, the water is modelled as a perfect tritium sink through a zero-T concentration BC, due to rapid isotopic exchanged between tritium and protium in the water molecule [3]. At the right boundary of the FLiBe domain a symmetry BC is used, modelling the geometric symmetry of the DWHX pipes. Finally, at the outlet of the fluid domains (FLiBe and helium) and at the top/bottom ends of the solid regions a *zeroGradient* BC ($\partial C/\partial n = 0$) is applied. The temperature profiles calculated by RELAP5, and discussed in Section 2.2, are imposed as fixed values in each region.

Tritium transport properties, i.e., diffusion coefficients and solubilities, depend on temperature according to the Arrhenius equation. Activation energies (E_a, kJ) and pre-exponential factors used for the different materials are shown in Table 5 and are obtained from [35] (FLiBe), from [31] (Hastelloy N) and from [36] (helium).

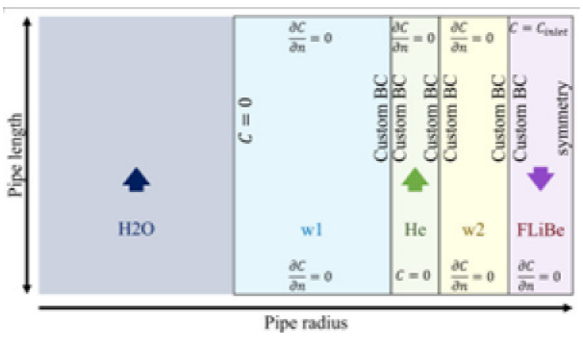

Fig. 5. DWHX OpenFOAM case geometry and tritium BCs.

For pressure-velocity coupling *chtMultiRegionFoam* uses a hybrid between the Pressure-Implicit with Splitting of Operators (PISO) algorithm and the Semi-Implicit Method for Pressure-Linked Equations (SIMPLE) algorithm, called PIMPLE [37]. The discretization schemes adopted in the simulations are first order for temporal discretization and second order for spatial discretization. The mesh is hexahedral, structured and coherent and a mesh sensitivity analysis has been conducted to ensure the independence of the results with respect to the computational grid resolution (this analysis will be presented in a dedicated paper). Convergence is evaluated through the monitoring of tritium fluxes between the interfaces and the solution is considered convergent when the relative deviation between two time steps is less than 1.0E-10 and all the residuals are below 1.0E-6.

4. Results

Fig. 6 shows the tritium concentration inside the different regions for the reference case (Table 1) normalized with respect to the FLiBe inlet value. The tritium loaded FLiBe enters the heat exchanger from the top (see Fig. 5). As it descends, tritium diffuses towards the w2 wall initially void of tritium and its concentration decreases going downwards near the interface between the two (Fig. 6-A). Here, due to the high solubility of tritium in the metal compared to the one in the FLiBe, the concentration exhibits a peak at the contact wall with FLiBe (Fig. 6-B). Subsequently, tritium diffuses into the helium and has a greater concentration towards the upper part of the pipe as it is in counterflow with the FLiBe (Fig. 6-C). Finally, tritium permeates into the w1 wall, concentrating more in the upper part where there is also a higher helium concentration (Fig. 6-D).

Fig. 7 shows the radial profile of the tritium concentration at the bottom, at the half-length and at the top of the HX tubes for all the cases analyzed (see Table 4). As also shown in Fig. 6, the greatest variations in the T_2 concentration occur when passing from one region to another, clearly visible through the "concentration jumps" at the interfaces, due to the high difference in the solubility of tritium in the different materials. The variation of the helium flow rate alters the temperature profiles within the HX, as shown in Fig. 4, and thus the tritium transport. When the helium flow rate is lower (S2 case), the average temperatures in metals and in helium, especially in the upper region of the DWHX, are significantly lower compared to the reference case (REF), due to the reduction of the average HTC (see Table 4). This leads to a lower diffusive flux from w2 towards helium which overall causes a higher concentration of tritium at the FLiBe outlet and a lower helium extraction efficiency, as shown in Table 6.

Finally, Table 6 summarizes the results obtained from OpenFOAM at steady state for the reference case and for varying helium velocity (Table 4). The overall release rate from one DWHX towards water with varying helium mass flow expressed in Ci/day is computed using tritium activity [38], tritium molecular weight and the value of release rate in mol/s. On the other hand, a lower helium flow rate means an increase of the residence time of the helium inside the HX and this leads to an higher concentration of tritium in all the tube length, as shown in Fig. 7 and in Table 6. The same conclusions are "mirrored" for the S3 case, where a

Table 5
Adopted tritium solubilities and diffusivities.

Parameter	E_a (kJ)	Pre-exp factor
D_{FLiBe} [m^2/s]	42	9.3E-07
K_{FLiBe} [mol/m^{3}Pa]	35	7.9E-02
$D_{Hastelloy\ N}$ [m^2/s]	56	1.69E-06
$K_{Hastelloy\ N}$ [mol/m^{3}Pa$^{0.5}$]	7.5	0.12
D_{He} [m^2/s]	8.998	4.13E-04
K_{He} [mol/m^{3}Pa]	6.340	5.79E-05

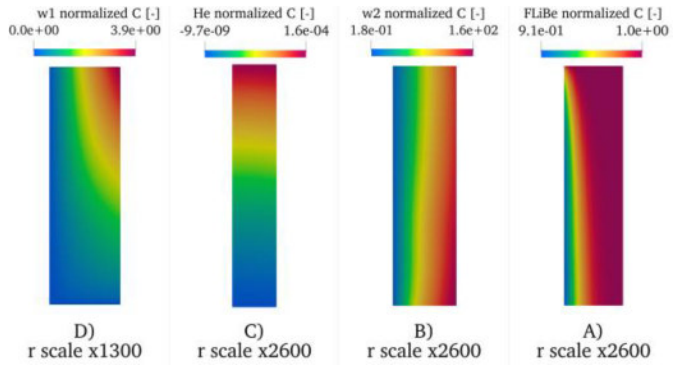

Fig. 6. REF case HX pipe radial slices, full length: tritium concentration. The overall length of the HX is considered and reported. The radial scale is altered (a high multiplicative factor is applied) to enhance the results readability.

greater velocity of the helium leads to a lower concentration of tritium in the helium (Fig. 7) but to a greater extraction due to the high velocity imposed (Table 6) and the different permeation flux from w2. Further analyses as the addition of a concentration of tritium higher than zero at the helium inlet, the addition of turbulence modelling and the comparison with a single-wall heat exchanger could be the object of a future work.

The HX extraction efficiency is computed as the ratio of the release rate to helium to the FLiBe inlet rate, instead the barrier efficiency is computed as the complement to one of the ratios between the release rate to water and the FLiBe inlet rate. The barrier efficiency is very similar for all cases, and it is higher for S2 due to the lower release rate to water compared to REF and S3.

As summarized in Table 6, the component effectively fulfills the function of a barrier for tritium concerning permeation in water for all tested configurations, with nearly unitary barrier efficiency values. However, it fails to serve as a tritium extractor, exhibiting extraction efficiencies of less than 1 %, as tritium diffusion in helium remains quite low regardless of its flow rate.

5. Conclusions

The preliminary sizing of a DWHX to be installed in an ARC-class fusion reactor primary cooling system has been performed. This goal was achieved through theoretical calculations verified with a RELAP5-3D© analysis. The adoption of a high helium flow rate allows the achievement of an acceptable height for the HX.

Then, a sensitivity analysis was carried out to optimize the component layout. Some solutions were identified to reduce the HX height, but they pose challenging issues to the component manufacturing (i.e., low bundle p/d that makes difficult the realization of the tubesheets).

Finally, tritium transport studies were performed to evaluate the DWHX performances as tritium barrier and extractor. The simulation results highlighted how the current preliminary design is not adequate to remove tritium for fuel recycling purposes, as the tritium extraction efficiency is very low. This is mainly due to the low permeation from FLiBe to helium. Instead, the component seems to correctly fulfill the tritium barrier function for all the scenarios considered, as the quantity of tritium reaching the secondary water varies from 7.5 to 12.0 E-03 Ci/day (three times the values in Table 6, referred to a single HX), well below the value preliminary assumed as reference for the release rate (~10 Ci/day) [5]. This leaves room for further optimizations of the DWHX layout, also evaluating the case in which a TES is inserted upstream the HX.

CRediT authorship contribution statement

Francesco Colliva: Writing – review & editing, Writing – original draft, Software, Resources, Methodology, Investigation, Formal analysis, Data curation, Conceptualization. **Federico Hattab:** Software, Formal analysis, Data curation, Conceptualization. **Simone Siriano:** Supervision. **Gabriele Ferrero:** Supervision. **Samuele Meschini:** Supervision. **Raffaella Testoni:** Supervision. **Massimo Zucchetti:** Supervision. **Andrea Iaboni:** Supervision. **Giulia Valeria Centomani:** Supervision. **Antonio Trotta:** Supervision. **Cristiano Ciurluini:** Supervision.

Table 6
DWHX T_2 permeation analysis - steady state results.

Parameter	Units	REF	S2	S3
FLiBe inlet C_{T2}	mol/m^3	1.36E-04		
Release rate to helium	mol/s	2.35E-07	1.90E-07	2.49E-07
Release rate to water	mol/s	8.64E-10	4.39E-10	8.42E-10
	Ci/day	5.74E-03	2.92E-03	5.60E-03
FLiBe outlet C_{T2}	mol/m^3	1.329E-4	1.334E-4	1.327E-4
Helium outlet C_{T2}	mol/m^3	2.09E-08	3.55E-08	1.24E-08
Efficiency (T_2 barrier)	%	99.997	99.998	99.997
Efficiency (T_2 extraction)	%	0.87	0.70	0.92

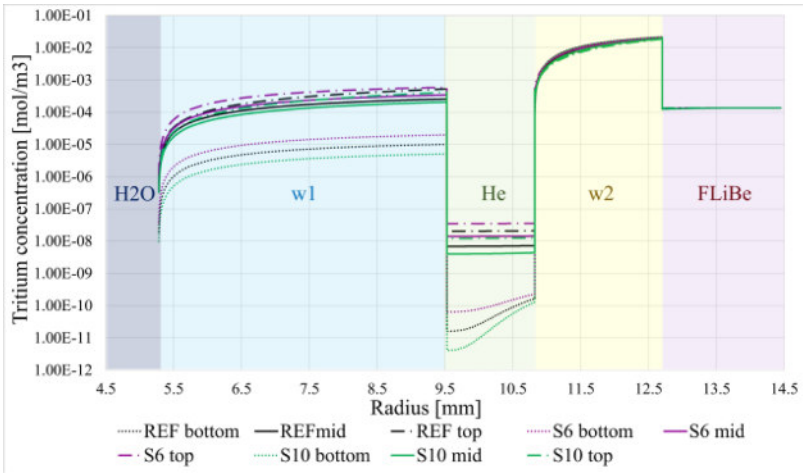

Fig. 7. T_2 concentration [mol/m3] radial trend inside a HX pipe at the base (bottom), at the half length (mid) and at the top of the pipe. Three cases at varying helium velocity (see Table 3 and Table 4) are shown.

Declaration of competing interest

The authors declare that they have no known competing financial interests or personal relationships that could have appeared to influence the work reported in this paper.

Data availability

No data was used for the research described in the article.

References

[1] B.N. Sorbom, et al., ARC: a compact, high-field, fusion nuclear science facility and demonstration power plant with demountable magnets, Fusion Eng. Des. 100 (2015) 378–405, https://doi.org/10.1016/j.fusengdes.2015.07.008.

[2] C.W. Forsberg, et al., Tritium control and capture in salt-cooled fission and fusion reactors: status, challenges, and path forward, Nucl. Technol. 197 (2017) 119–139, https://doi.org/10.13182/NT16-101.

[3] C. Forsberg, G. Zheng, R.G. Ballinger, S.T. Lam, Fusion blankets and fluoride salt cooled high temperature reactors with flibe salt coolant: common challenges, tritium control, and opportunities for synergistic development strategies between fission, fusion and solar salt technologies, Nucl. Technol. 206 (2020) 1778–1801, https://doi.org/10.1080/00295450.2019.1691400.

[4] S. Segantin, et al., Exploration of power conversion thermodynamic cycles for ARC fusion reactor, Fusion Eng. Des. 155 (2020) 111645, https://doi.org/10.1016/j.fusengdes.2020.111645.

[5] S. Fukada, et al., Tritium recovery system for Li-Pb loop of inertial fusion reactor, Fusion Eng. Des. 83 (2008) 747–751, https://doi.org/10.1016/j.fusengdes.2008.05.030.

[6] S. Meschini, et al., Modeling and analysis of the tritium fuel cycle for ARC-and STEP-class DT fusion power plants, Nucl. Fusion 63 (12) (2023) 126005, https://doi.org/10.1088/1741-4326/acf3fc.

[7] S. Zhang, et al., A coupled heat transfer and tritium mass transport model for a double-wall heat exchanger design for FHRs, Ann. Nucl. Energy 122 (2018) 328–339, https://doi.org/10.1016/j.anucene.2018.08.039.

[8] B.M. Wallace, Analysis of double-wall and twisted-tube heat exchanger concepts for use in fluoride salt-cooled high-temperature reactors (2018). Available online at: https://digitalrepository.unm.edu/ne_etds/93/.

[9] RELAP5-3D© Code Manual, The RELAP5-3D Code Development Team, 2013. INEEL-EXT-98-00834.

[10] C.J. Greenshields, OpenFOAM v9 User Guide, The OpenFOAM Foundation, London, UK, 2021. Available online at: https://doc.cfd.direct/openfoam/user-guide-v9.

[11] S. Cantor et al., Physical properties of molten-salt reactor fuel, coolant, and flush salts, Oak Ridge Report No.: ORNL-TM-2316, 1968.

[12] The International Association for the Properties of Water and Steam (IAPWS), in: Revised Release on the IAPWS Industrial Formulation 1997 for the Thermodynamic Properties of Water and Steam, Lucerne, Switzerland, 2007. AugustAvailable online at: http://www.iapws.org/relguide/IF97-Rev.pdf.

[13] V.D. Arp, et al., Thermophysical Properties of Helium-4 from 0.8 to 1500 K With Pressures to 2000 MPa, National Institute of Standards and Technology, 1998.

[14] F. Dittus, L. Boelter, Heat transfer in automobile radiators of the tubular type, Int. Commun. Heat Mass Trans. 12 (1985) 3–22, https://doi.org/10.1016/0735-1933(85)90003-X.

[15] V. Gnielinski, New equations for heat and mass transfer in turbulent pipe and channel flow, Int. J. of Chem.Eng. 16 (1976) 359–368.

[16] C. Ciurluini, et al., Study of the eu-demo wcll breeding blanket primary cooling circuits thermal-hydraulic performances during transients belonging to lofa category, Energies 14 (6) (2021) 1541, https://doi.org/10.3390/en14061541.

[17] C. Ciurluini, et al., Thermal-hydraulic modeling and analysis of the Water Cooling System for the ITER Test Blanket Module, Fusion Eng. Des. 158 (2020) 111709, https://doi.org/10.1016/j.fusengdes.2020.111709.

[18] G.R. Longhurst, D. Holland, J. Jones, B. Merrill, Tmap4 Users Manual, EG and G Idaho, Inc.,, Idaho Falls, ID (United States),, 1992 tech. rep.

[19] J. Ambrosek, Verification and Validation of Tmap7, ,Idaho National Lab.(INL), Idaho Falls, ID (United States), 2008 tech. rep.

[20] F. Waelbroeck, P. Wienhold, J. Winter, E. Rota, T. Bauno, Influence of bulk and surface phenomena on the hydrogen permeation through metals, tech. rep, ., Kernforschungsanlage Juelich GmbH (1984). Germany.

[21] A. Pisarev, K. Miyasaka, T. Tanabe, Permeation of hydrogen through tantalum: influence of surface effects, J. Nucl. Mater. 317 (2–3) (2003) 195–203, https://doi.org/10.1016/S0022-3115(03)00079-5.

[22] H. Carslaw and J. Jaeger, "Conduction in heat and solids second edition," p. 60, 1959.

[23] J. Crank, The Mathematics of Diffusion, Oxford university press, 1979.

[24] S. Fukada, A. Morisaki, Hydrogen permeability through mixed molten salt of LiF, NaF and KF (Flinak) as a heat-transfer fluid, J. Nucl. Mater. 358 (2–3) (2006) 235–242, https://doi.org/10.1016/j.jnucmat.2006.07.011.

[25] P. Calderoni, P. Sharpe, M. Hara, Y. Oya, Measurement of tritium permeation in FLiBe (2LiF-BeF2), Fusion Eng. Des. 83 (7–9) (2008) 13311334, https://doi.org/10.1016/j.fusengdes.2008.05.016.

[26] R. Macaulay-Newcombe, D. Thompson, W. Smeltzer, Deuterium diffusion, trapping and release in ion-implanted beryllium, Fusion Eng. Des. 18 (1991) 419424, https://doi.org/10.1016/0920-3796(91)90158-M.

[27] J.D. Stempien, Tritium transport, corrosion, and Fuel Performance Modeling in the Fluoride Salt-Cooled High-Temperature Reactor (FHR), Massachusetts Institute of Technology, 2015. PhD thesis.

[28] A.D. Lindsay, USDOE Office of Nuclear Energy (NE). TMAP8. Computer Software, 2021, https://doi.org/10.11578/dc.20210205.2. https://github.com/idaholab/TMAP8, 04 JanWeb.

[29] P.-C.A. Simon, P.W. Humrickhouse, A.D. Lindsay, Tritium transport modeling at the pore scale in ceramic breeder materials using tmap8, IEEE Transact. Plasma Sci. 50 (11) (2022) 44654471, https://doi.org/10.1109/TPS.2022.3183525.

[30] F. Hattab, et al., An OpenFOAM multi-region solver for tritium transport modeling in fusion systems, Fus. Eng. Des. (2023) submitted.

[31] T.F. Fuerst, et al., Tritium Transport Phenomena in Molten-Salt Reactors: Molten Salt Tritium Transport Experiment Design. No. INL/EXT-21-63108-Rev000, Idaho National Lab.(INL), Idaho Falls, ID (United States), 2021. Available online at: https://www.osti.gov/biblio/1828384.

[32] A.P. Malinauskas, et al., The solubility of hydrogen, deuterium and helium in molten Li2BeF4, Ind. Eng. Chem. Fundam. 13 (1974) 242–245, https://doi.org/10.1021/i160051a015.

[33] F. Reiter et al., A compilation of tritium /material interaction parameters in fusion reactor materials, EUR 15217 EN (1993).

[34] G. Ferrero, et al., A Preliminary CFD and Tritium Transport Analysis for ARC, Fusion Sci. Technol. 78 (2022) 617–630, https://doi.org/10.1080/15361055.2022.2096365.

[35] P. Calderoni et al., Measurement of tritium permeation in flibe (2LiF-BeF2), Fusion Eng. Des., vol. 83, pp. 1331–1334. https://doi.org/10.1016/j.fusengdes.2008.05.016.

[36] S. Zhang, et al., A coupled heat transfer and tritium mass transport model for a double-wall heat exchanger design for FHRs, Ann. Nucl. Energy 122 (2018) 328–339, https://doi.org/10.1016/j.anucene.2018.08.039.

[37] C.J. Greenshields, et al., Notes On Computational Fluid Dynamics: General Principles, CFD Direct Ltd, Reading, UK, 2022.

[38] Physical and chemical properties of tritium. Available at: https://www.nrc.gov/docs/ML2034/ML20343A210.pdf.